Feature

Equalization in High-Speed Communication Systems

Jin Liu and Xiaofeng Lin

© EYEWIRE

Abstract

The article first discusses the major non-ideal issues of low-cost transmission media for over Gbps data transmissions—the frequency dispersion loss and channel noise. The former causes ISI in received signal, which presents difficulty for clock and data recovery at high frequencies and results higher BER. The latter further degrades the received signal quality and further limits the data transmission rate and transmission distance. Then, two equalization approaches—transmitter pre-emphasis and receiver equalization, are reviewed, in addition to various adaptation criteria and algorithms.

 1540-7977/04/$20.00©2004 IEEE

Authorized licensed use limited to: WASHINGTON UNIVERSITY LIBRARIES. Downloaded on March 25,2025 at 20:42:53 UTC from IEEE Xplore. Restrictions apply.

Volex Exhibit 1048
Volex v. Credo

Introduction

Communication systems may be described by the block diagram shown in Figure 1. They always involve three basic parts: the transmitter (TX), the channel, and the receiver (RX). The signal, $s(t)$, is the transmitted signal and the signal, $r(t)$, is the received signal. Non-ideal channel characteristics, for example, limited channel bandwidth and crosstalk noise, often deteriorate the signal quality of the received signal and causes error in data recovery.

For example, Figure 2 illustrates that a band limited channel causes inter-symbol-interference (ISI). The top trace is the transmitted signal, which is a binary digital signal composed of "1"s and "0"s; the bottom trace is the received signal. When the transmitted data has a long string of "1"s, followed by single "0" at location A and B, the effect of ISI is very significant as circled. The "0" following the three "1" is very close to the reference voltage, which is defined as the middle voltage between the binary voltage levels. When there is additional noise presented in the channel, this "0" code will very likely be misinterpreted as a "1" code and this causes higher bit error rate in data recovery.

In addition to the data recovery error, ISI together with other non-ideal characteristics of the channel also cause difficulty in clock and data recovery (CDR) at high frequencies. This can be illustrated by the eye diagram shown in Figure 3. The eye diagram can be viewed on an oscilloscope by displaying the signal on the vertical input with horizontal sweep rate set at multiples symbol rate frequency. Eye diagram is also called eye-pattern because its resemblance to human eyes. Figure 3(a) shows the eye diagram of the transmitted signal, which is the same signal shown in Figure 2. It has wide open eyes and the clock information can be easily recovered. However, the eye diagram of the received signal shown in Figure 3(b) has closed eyes and timing jitter is very severe. Clock and data recovery is impossible and equalization is mandatory to restore the timing information in this case. In summary, equalization is used to improve the received signal quality for correct clock and data recovery, so that the system achieves lower bit error rate for the goal of error-proof data communications.

There are various communication channels with distinct channel characteristics. Some examples are: air, vacuum, seawater, twisted pair telephone lines, coaxial cables, waveguides, printed circuit board (PCB) traces, fiber-optics cables, and magnetic read/write channels. A classical equalization application is sending fax through the telephone line; the connection tones we hear at the beginning of sending fax are for the purpose of equalization. The path connecting two phone terminals is different depending on the phone number; even with the same

Figure 1. Basic components of a communication system.

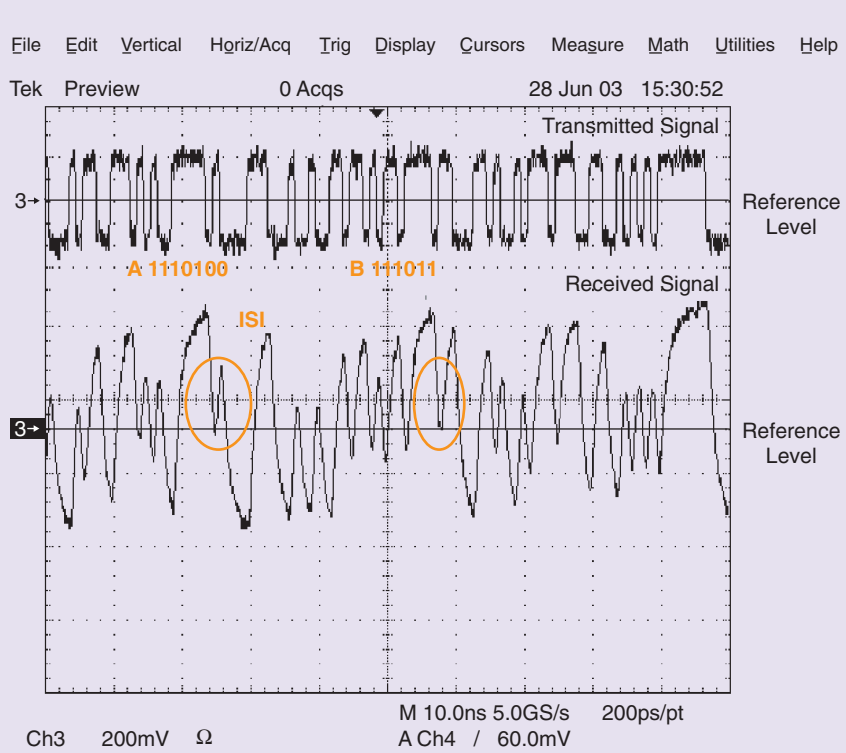

Figure 2. Illustration of ISI—the transmitted signal (top) and the received signal (bottom) through a band limited channel.

Jin Liu and Xiaofeng Lin are with the Department of Electrical Engineering, the University of Texas at Dallas, P.O. Box 830688, EC 33, Richardson, TX 75083-0688 USA. Phone: 972-883-4393; Fax: 972-883-2710; E-mail: jinliu@utdallas.edu.

Authorized licensed use limited to: WASHINGTON UNIVERSITY LIBRARIES. Downloaded on March 25,2025 at 20:42:53 UTC from IEEE Xplore. Restrictions apply.

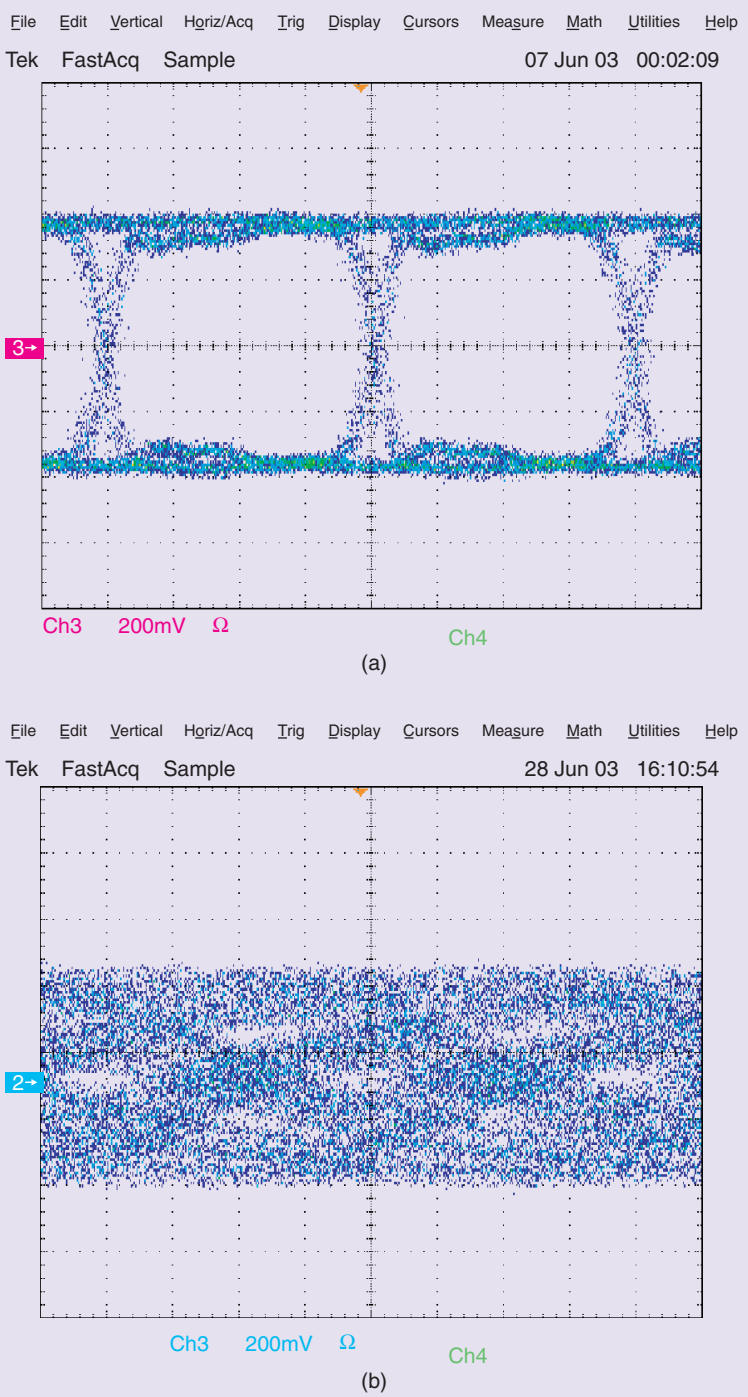

Figure 3. Eye diagram of (a) the transmitted signal and (b) the received signal.

phone number, the switch network might connect them differently each time depending on the traffic. Thus, in this case, training sequences known to both TX and RX are transmitted; the channel characteristics can be computed by comparing the known training sequence with the actual received signal. Other typical examples are Ethernet communications with transmission rate of several hundred Mbps [1], where over 100 meters of transmission distance causes severe channel loss, and the magnetic read/write channels for hard disk drives [2] with speed around 500 Mbps, where adjacent track causes severe ISI at high storage densities. With the increasing demand for higher speed processing, the data rate in chip-to-chip communications for back plane, front plane, personal and mainframe computer has been pushed to several Gbps range and even beyond 10 Gbps range. At this frequency range, the low-cost printed circuit board (PCB) trace introduces significant attenuation to the signal; equalization has become mandatory to ensure reasonable transmission distance. Due to the limited bandwidth of the PCB trace material, optical channel has been considered for beyond 10 Gbps data transmission for above chip-to-chip applications. Currently, the main barriers are high cost, lower degree of integration, and complexity of the implementation. For optical communications, the ISI is caused by polarization mode dispersion (PMD), chromatic dispersion (CD), and other impairments [3]; electronic equalizer at 10 Gbps has also been used as an effective solution [4].

In this article, we will first introduce, in section Metalic Channel Loss, the frequency dependent loss of metallic channel, specifically the PCB media for over Gbps data transmissions, then, in section Inter-symbol Interference, ISI as a result of channel loss will be explained. In section Crosstalk, the major noise source—crosstalk noise in high-speed communication system is briefly discussed and in section Pulse Modulation, the widely used pulse modulation schemes are reviewed. There are two types of equalization schemes: one is at the transmitter side, as reviewed in section Transmitter Pre-emphasis; the other is at the receiver side, as reviewed in section Receiver Equalizer. As mentioned earlier, the communication channel characteristics vary and adaptive equalization is generally required. Section Adaptation Criteria and Related Algorithmus will discuss the adaptation schemes for high-speed equalizers.

Authorized licensed use limited to: WASHINGTON UNIVERSITY LIBRARIES. Downloaded on March 25,2025 at 20:42:53 UTC from IEEE Xplore. Restrictions apply.

Metallic Channel Loss

For PCB channel in chip-to-chip communications, there are mainly two non-ideal characteristics that limit the data transmission rate and distance. The first is the limited bandwidth due to frequency dependent channel loss; the second is cross talk. For all metallic media, including PCB traces and metallic cables like unshielded twist pair (UTP) cables, shielded twisted pair (STP) cables and coaxial cables, the channel losses at higher frequencies are mainly caused by skin effect and dielectric loss [5, 6]. Other loss scheme like radiation loss is negligible even when the signal frequency is up to 10 GHz. When high-frequency signal flows through metallic media, the induced magnetic field causes the current to flow only on the conductor surface and current density decreases exponentially toward the interior. This phenomenon is called skin effect. Dielectric loss is the loss of electromagnetic power due to the non-ideal characteristics of the dielectric material as isolator around the conducting media during electromagnetic wave propagation. The channel loss due to these two factors can be expressed by the following equation [6]:

$$C(f) = e^{-[h_s(1+j)\sqrt{f}+h_d f]l},$$

where h_s is skin-effect loss coefficient, h_d is dielectric loss coefficient, l is length of the media, and f is frequency. Figure 4 shows the measurement of the channel loss, specifically it is the S21 parameter of a single-ended 180-inch PCB microstrip with two SMT connectors. The trace width affects the loss characteristics; a wider trace introduces smaller attenuation.

Both the equation and the plot show that the channel loss increases with frequency, specifically, the attenuation due to skin effect increases exponentially with the square root of frequency and the attenuation due to dielectric loss increases exponentially with frequency. Thus, the metallic transmission media have limited bandwidth which limits the data transmission rate. Also shown in the equation is that the channel loss increases exponentially with media length, as a result, the data transmission has limited transmission distance. Indeed, the equation shows that there is a trade off between the transmission rate and the transmission distance. For the same media, if the transmission distance is shorter, it is possible to transmit at higher data rate. Each different media has its own unique skin effect coefficient and the dielectric loss coefficient. For example, the UTP cables widely used for building wiring have larger attenuation coefficients than those of the coaxial cables.

Figure 4 shows that at 1 GHz, the channel loss for this trace is about 25 dB. The signals shown in Figure 2 and Figure 3 are for data transmission through this channel at data rate 1 Gbps. When the channel loss is the only non-ideal factor being considered, the loss characteristics can be identified by the channel loss at symbol rate frequency; for 1 Gbps data rate, the corresponding symbol rate frequency is 1 GHz. When the channel attenuation is about 25 dB at symbol rate frequency, the channel loss is quite severe and it causes the received signal to have closed eyes.

Inter-symbol Interference

The channel transfer function in the previous section shows that different frequency suffers different degrees of attenuation and phase delay. A transmitted square wave

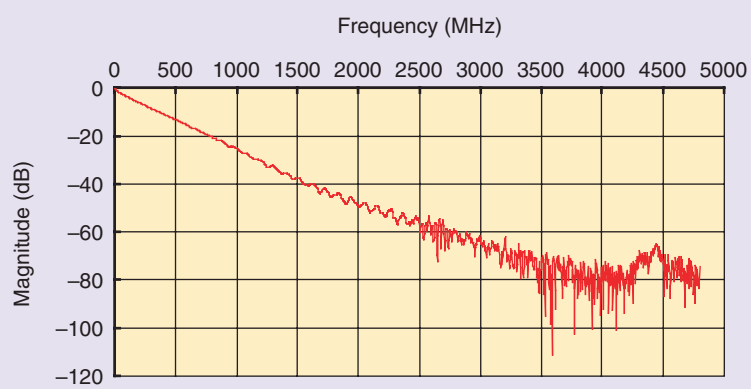

Figure 4. Measured S21 parameter for a PCB trace.

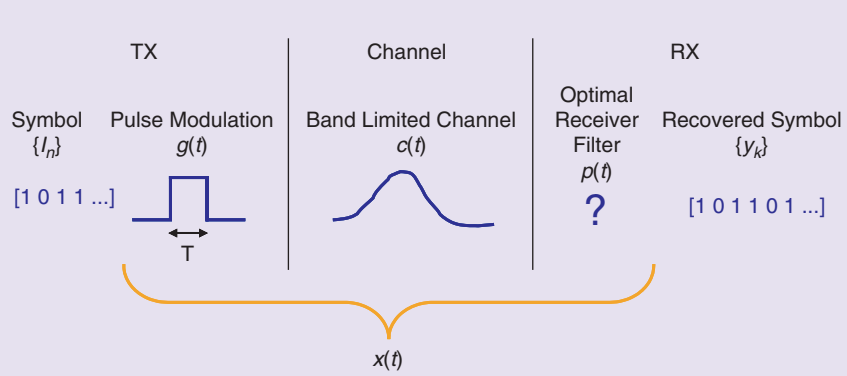

Figure 5. Communication channel with transmitter pulse modulation and receiver filter.

Authorized licensed use limited to: WASHINGTON UNIVERSITY LIBRARIES. Downloaded on March 25,2025 at 20:42:53 UTC from IEEE Xplore. Restrictions apply.

contains many frequency components, after transmission through the channel, the frequency components suffer dispersion due to different degrees of magnitude attenuation and phase delay. Due to similar dispersion effect on light, we see the appearance of rainbow.

The term of inter-symbol interference describes the dispersion effect in discrete time domain, where the transmitted data are treated as digital symbols with pulse modulation. Figure 5 shows the communication channel with transmitter pulse modulation and receiver filter. For binary data, which is also know as two level pulse amplitude modulation (2-PAM) shown in Figure 2, the discrete information-bearing symbol $\{I_n\}$ is either "1" or "0" and the modulation pulse is a square pulse as shown.

For several types of digital modulation techniques, including 2-PAM, the received signal after the receiver filter, without considering channel noise, can be expressed as [7]

$$y(t) = \sum_{n=0}^{\infty} I_n x(t - nT)$$

where x(t) is the overall response including the transmitter modulation, channel function, and receiver filter. To obtain the recovered symbol, $y(t)$ is sampled at times $t = kT + \tau_0, k = 0, 1, \ldots,$ where τ_0 is the transmission delay. We then have

$$y(kT + \tau_0) \equiv y_k = \sum_{n=0}^{\infty} I_n x(kT + \tau_0 - nT)$$

or equivalently,

$$y_k = \sum_{n=0}^{\infty} I_n x_{k-n} = x_0 I_k + \sum_{\substack{n=0 \\ n \neq k}}^{\infty} I_n x_{k-n}$$

The term $x_0 I_k$ represents the desired information symbol at the kth sampling point and the term $\sum_{\substack{n=0 \\ n \neq k}}^{\infty} I_n x_{k-n}$ represents ISI.

If the channel has infinite bandwidth, the channel impulse response is an impulse, $\delta(t)$. Because of bandwidth limitation, the channel impulse response, $c(t)$, is a spread pulse as shown in the above figure. Convolving the modulation pulse, $g(t)$, with $c(t)$ results an impulse response whose pulse width is wider than T, the pulse width of $g(t)$. The receiver filter is usually designed as match filter. Without equalization filter in the receiver filter, the overall impulse response $x(t)$ will have wider pulse width than T, as illustrated in the top plot in Figure 6. The bottom plot in the same figure shows that four consecutive symbols of "1"s are transmitted. Looking at the sampling point KT, the recovered symbol is the sum of the desired symbol value labeled by point 0; it equals x_0 on curve C, plus ISI from neighboring symbols, namely point 1 from curve B ($=x_1$), point 2 from curve A ($=x_2$) and point 3 from curve D ($=x_{-1}$). In summary, ISI occurs when the overall impulse response, $x(t)$, has wider spread than the symbol period T.

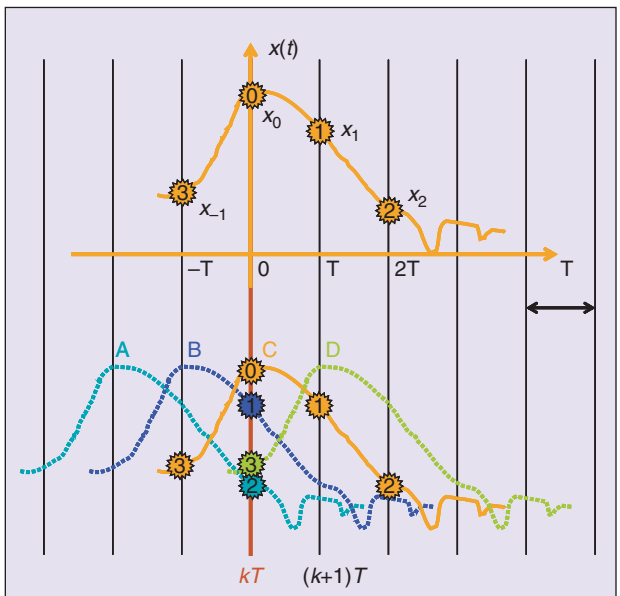

Figure 6. Illustration of ISI.

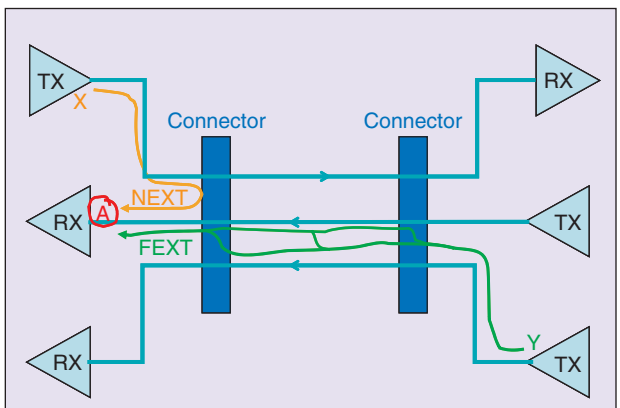

Figure 7. Illustration of NEXT and FEXT.

Crosstalk

In addition to the channel loss non-ideal characteristic, there are various noise sources that cause errors in data and clock recovery, for example, the crosstalk noise, the power supply noise, and reflection noise. Crosstalk is caused by the electromagnetic coupling between signal lines through mutual capacitance and mutual inductance. Power supply noise is induced by switching large currents in short duration across the parasitic inductance in power distribution network; it increases with the switching frequency of I/O driver, output signal swing, and number of switching drivers at the same time. Reflections are

Authorized licensed use limited to: WASHINGTON UNIVERSITY LIBRARIES. Downloaded on March 25,2025 at 20:42:53 UTC from IEEE Xplore. Restrictions apply.

due to impedance discontinuities; common reflection noise for backplane applications includes card-to-board connectors, cable-to-card connectors, long vias with their respective end pads, wire bonds or flip-chip solder balls and orthogonal wiring [8, 9].

Among the various noise factors, the dominant one for backplane is the crosstalk noise, specially the near end cross talk (NEXT) at the connectors. Figure 7 illustrates the near end crosstalk and the far end crosstalk (FEXT). For the receiver at point A, the crosstalk generated from nearby transmitter at point X is the NEXT. In this figure, only the major coupling path—through the connector, is illustrated. In reality, the PCB traces between the two connectors also contribute for NEXT. The FEXT is generated from transmitter at the other end, point Y in the figure. As NEXT, FEXT also has multiple paths. Since the FEXT transfer channel has much longer distance than that of NEXT, the FEXT transfer function has much more severe attenuation than the NEXT transfer function. Therefore, NEXT is more critical to correct data recovery of weak received signal in receiver end. The NEXT transfer function increases with frequency [10, 11]. For high-speed data transmissions, effective equalization method to mitigate the NEXT has become necessary.

Pulse Modulation

Currently, the most popular pulse modulation scheme for high-speed transceivers is the binary NRZ (2-PAM) with 8 b/10 b coding and scrambling. The data throughput rate can be improved by increasing the symbol rate or by using multilevel pulse modulation schemes like 4-PAM and 8-PAM as illustrated in Figure 8. For the same data throughput, the 4-PAM scheme transmits data at half the rate 2-PAM scheme. This is advantageous since the channel loss is smaller at lower frequencies. However, 4-PAM schemes that employ symbols $\{-1, -3\}$ suffer from the increased energy due to symbols -3, and from having to use three thresholds to separate the symbols. Specifically, a 4-PAM scheme requires an average energy 5 times as much as a binary scheme, which has a significant impact on detection. If the same maximum amplitude is maintained, the separation between adjacent symbol amplitudes (we define it as symbol amplitude here) in 4-PAM is 1/3 of binary signaling, which results in about a 9.5 dB loss in symbol power. As a result, multilevel coding schemes reduce the data transmission rate, at the price of reducing received symbol power. It is desirable to search for binary schemes that can increase the transmission rate without expanding the signal bandwidth.

The power spectrum density of widely used binary NRZ scheme resembles the shape of a $sinc^2$ function. For example, Figure 9 shows the magnitude of the Fourier transform of a random 2 Gbps 8 b/10 b coded NRZ data sequence. There is a null frequency at the symbol rate frequency, 2 GHz.

Transmitter Pre-emphasis

There are two types of equalization: transmitter pre-emphasis and receiver equalization. Both seek to either emphasize the high-frequency components or to de-emphasize the low frequency components of the transmitted or received signal, in order to compensate the effect that the high-frequency components are attenuated more than the low-frequency components through the channel. Using both the transmitter and receiver equalization allows the best system performance in terms of BER.

The transfer function of both types of equalizer is a high-pass filter; though in practice, it is a band-pass filter. One reason is that the bandwidth limitation of semiconductor devices cannot achieve infinite bandwidth; the other is to avoid noise amplification. Though the spectrum of transmitted signal is infinite, the main slope within the symbol rate frequency contains most of the

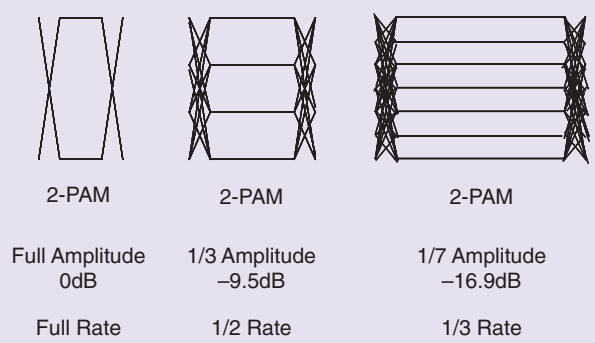

Figure 8. Multilevel signaling schemes.

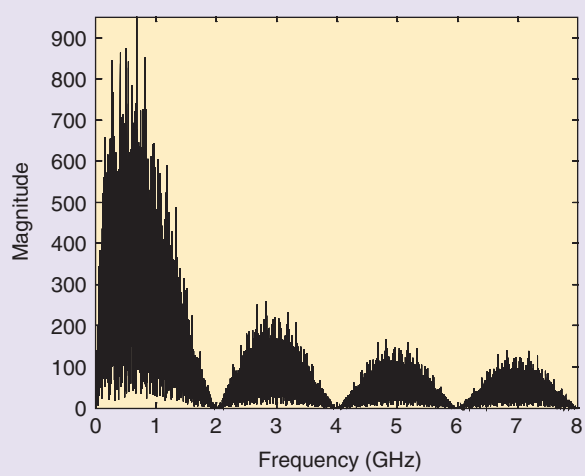

Figure 9. Frequency spectrum of the transmitted signal.

Authorized licensed use limited to: WASHINGTON UNIVERSITY LIBRARIES. Downloaded on March 25,2025 at 20:42:53 UTC from IEEE Xplore. Restrictions apply.

information, as shown in Figure 9. With additive white Gaussian noise (AWGN) and crosstalk noise, there is significant amount of noise beyond the symbol rate frequency bandwidth. If the equalizer still has significant gain after this bandwidth, the high-frequency noise will be amplified and it deteriorates the signal quality.

Pre-emphasis [12–16] is realized at the transmitter side. In some cases it increases the high-frequency components, which can cause EMI and more severe crosstalk problems. In other cases it reduces the power of low frequency components, known as de-emphasis. FIR filters are generally used for transmitter pre-emphasis. A simplified approach is to use two differential amplifiers, with the first one controlled by the original code, and the second by emphasis code (produced by inverting the original code and delay one symbol period). In some cases, the FIR filter was approximated by a transition filter implemented with a look-up table.

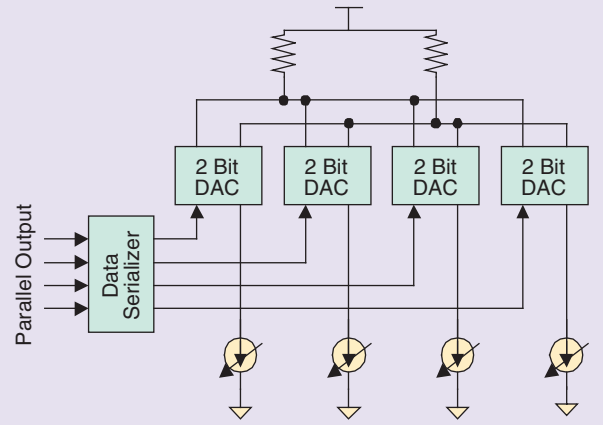

Figure 10. 4 tap FIR filter for transmitter pre-emphasis.

Figure 10 shows the block diagram of 4-tap sparse FIR filter for pre-emphasis equalizer with 4-PAM scheme [12]. Four 2-bit digital-to-analog converters (DAC) serve as the multiplier for FIR filter, whose input signal come from the data serializer. The 2-bit resolution is due to 4-PAM scheme. The FIR coefficients are set by controlling the steering current of 2 bit DACs using other four 6-bit DACs. Output currents of four MDACs are summed up at their output node and converted to voltage through off-chip 50 ohm resistors.

When parallel data are not present, the tap delay line can be simply realized with digital delay unit without need for high-speed ADC or analog tap delay line as in FIR filter of receiver end [17]. Figure 11 shows a block diagram of transmitter equalizer realized as 4-tap transversal FIR filter. Each FIR filter contains four 2-bit DAC modules, (again due to 4-PAM scheme), which correspond to four taps of FIR filter. The first DAC is the main tap and its output is proportional to the current output signal. Other three taps, whose inputs are one symbol to three symbols delay separately, compensate for the post-cursor ISI. All five FIR filters also serve as a 5:1 output multiplexer. They are toggled consecutively with 10 equal spaced clocks at each symbol period.

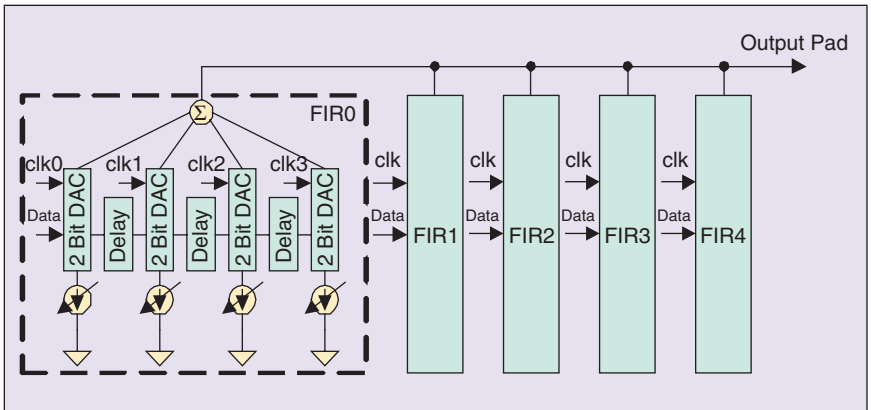

Figure 11. Block diagram of 4-tap transmitter equalizer.

Transmitter equalizer can also be a de-emphasis filter which reduces the power of low frequency component in advance. The simplest way to implement is increasing the signal amplitude at each transition edge and reducing the signal amplitude when there is no transition. In [14], the de-emphasis equalizer uses the inverted signal of previous bit as emphasis signal. During '0' to '1' transition edge, signal amplitude is increased; in '1' to '0' transition edge, signal amplitude is further increased to negative direction. In other periods when there is no transition, the emphasis signal is opposite to the current bit and signal amplitude is reduced. To better control the strength of pulse, the auxiliary 3-bit DACs can be used to set the emphasis level

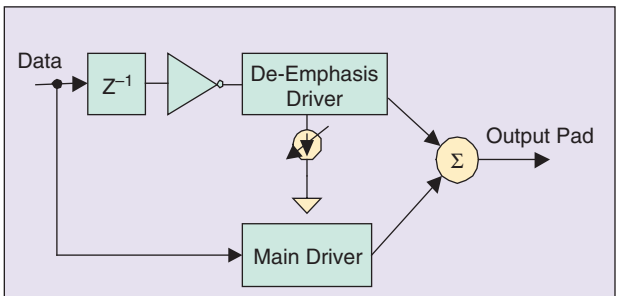

Figure 12. Block diagram of de-emphasis equalizer.

Authorized licensed use limited to: WASHINGTON UNIVERSITY LIBRARIES. Downloaded on March 25,2025 at 20:42:53 UTC from IEEE Xplore. Restrictions apply.

[15]. Figure 12 shows the block diagram of de-emphasis equalizer. This de-emphasis is actually a 2-tap FIR filter with a high-pass frequency response. Figure 13 illustrates the effect of de-emphasis.

The implementation of transmitter equalizer using FIR filter is relatively easier than that at the receiver side, because the parallel data bus naturally supplies the data input for FIR filter. However, the use of de-emphasis decreases the total transmitting signal power; as a result, decreasing the SNR at the receiver. In addition, since pre-emphasis is at the transmitter side, no channel characteristics information is present. Thus, it needs information sent from the receiver for dynamic or fine-tuned equalization, with special encoding packet or side band signaling. Alternatively, fixed amount of pre-emphasis can be used without consideration of the channel characteristics; the purpose of pre-emphasis is to improve in certain degree the received signal quality. The adaptation to varying channel characteristics is left to the receiver equalizer. Receiver equalizer can be adapted to the channel length, temperature and process variation. It can also incorporate complicated signal processing technique to increase bit error rate, such as using DSP-based processing, Viterbi decoder and partial response signaling. However, designing a GHz range filter or analog to digital converter (ADC) remains a challenging task.

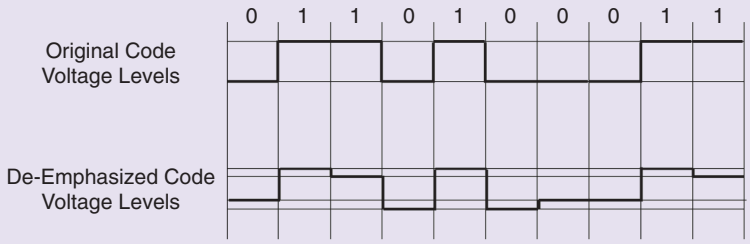

Figure 13. Illustration of de-emphasis.

Receiver Equalizer

There are generally four categories of receiver equalizers for over Gbps data transmissions: passive-component equalizer, active continuous-time equalizer using split-path amplifier, active equalizer using discrete-time FIR filter and active equalizer using continuous-time FIR filter.

Passive Receiver Equalizer

Figure 14 shows an implementation of a passive equalizer using bridged-T similar network [18]. Passive components in the equalizer define frequency characteristics in different band independently, which eases the design procedure. For example, R3, R4, R5 and L2 set the characteristics impedance; C2 and R2 set the low frequency compensation; mid-band frequency compensation is set by L2; and L1 and C1 set the high frequency compensation. Fixed passive equalization is easy to implement, it can work in a wide bit rate range and has low power consumption. However, the implementation highly depends on the coding scheme, it is sensitive to the model and process variation and has low SNR level and narrow compensation range. Passive equalizer is preferred in the case when the received signal has large amplitude and the receiver sensitivity is high.

Active Continuous-time Equalizer Using Split-path Amplifier

Split-path amplifier divides the signal path into two paths [19]. One path comprises a high pass filter or peak response filter to amplify the high frequency component. Another path is an all pass filter or a low pass filter to match the time delay of first path. Weighted sum of two paths is equivalent to a variant gain high pass filter, whose gain factor can be varied by control the weight of those two paths. Figure 15 shows a 3.2 Gbps adaptive cable equalizer using a peak response filter which is also a feedforward amplifier as it is equivalent to add a zero or a feed-ward path [20]. An equalizer control circuit compares the power ratio at two specific frequency

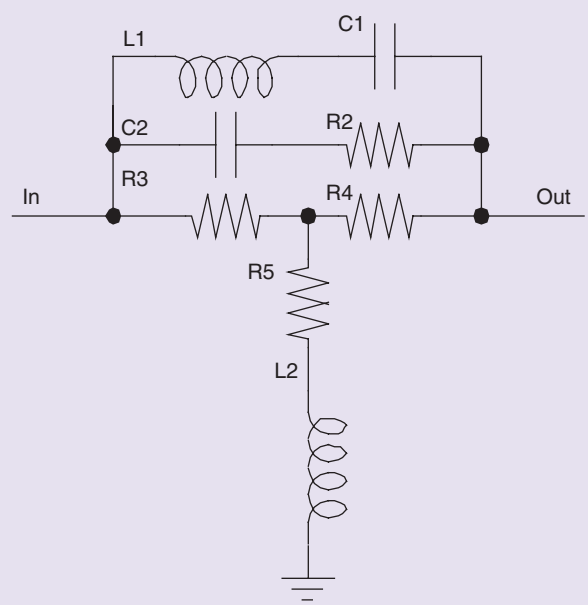

Figure 14. Passive T-bridge equalizer.

Authorized licensed use limited to: WASHINGTON UNIVERSITY LIBRARIES. Downloaded on March 25,2025 at 20:42:53 UTC from IEEE Xplore. Restrictions apply.

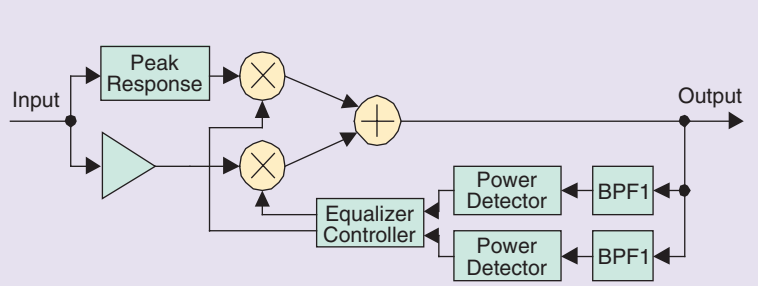

Figure 15. Split-path equalizer.

points using bandpass filters to set the weighted factor of those two paths.

To better match phase delay in split-path amplifier, the flat response path must use the same amplifier as in the feedforward path. Wider gain control range is achieved by jointly adjusting the poles position in both paths [21]. Traditional OPAMP-based amplifier using feedback resistor provides precise gain and low nonlinearity [1]. However, negative feedback loop prevents the amplifier working in GHz range. Phase mismatch between feedback loop and input signal also limit using a feedback loop amplifier in high frequency range. Figure 16 shows a wide band split-path amplifier without feedback loop; the amplifier gain is controlled through the load resistor instead of using feedback resistor.

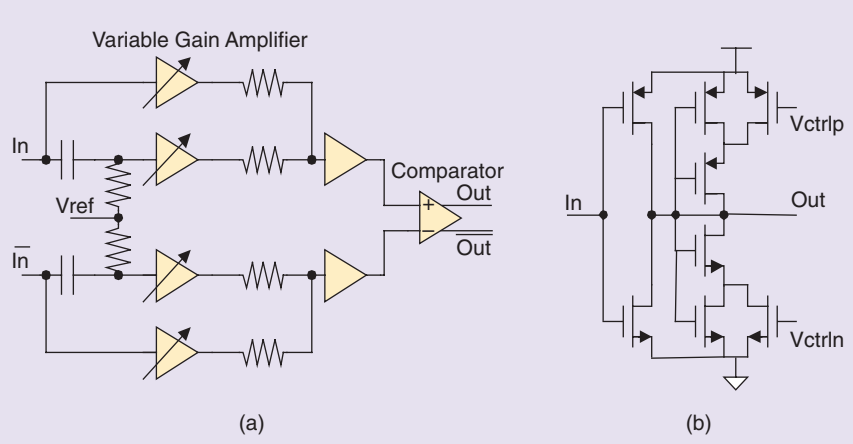

Figure 16. (a) Wideband split-path amplifier without feedback loop and (b) variable gain amplifer.

It is known that the transconductance of a source degeneration transconductor is close to the conductance, 1/R of the degeneration resistor [22]. If the degeneration comprises a resistor and a capacitor, the resistor corresponds to an all path loop while the capacitor corresponds to a high pass path. Therefore, such a transconductor cell serves as a compact split-path amplifier. To tune the high frequency gain and low frequency gain, the capacitor and resistor are implemented with varactor and a linear MOS transistor. Figure 17 shows the schematic of the source degeneration transconductor [23, 24]. Varying the controlling voltage of varactor and MOS transistor, *Vctrl* and *gmctrl*, will change the high frequency boosting and low frequency gain.

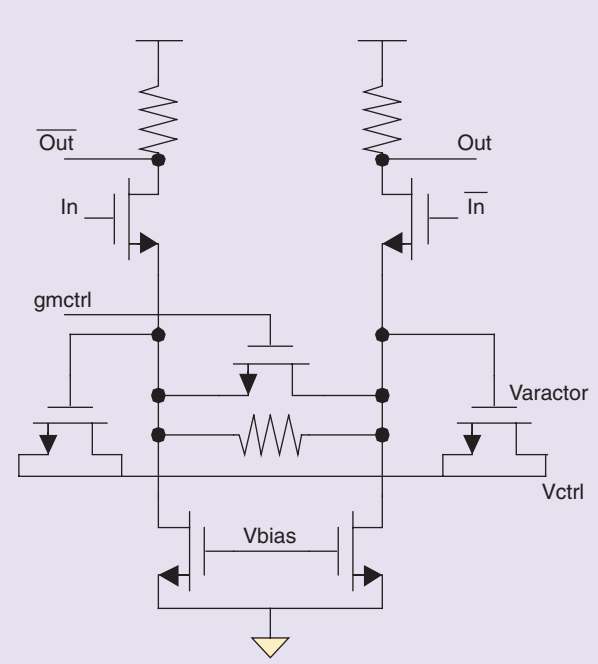

Figure 17. Source degeneration transconductor filter.

Active Equalizer Using Discrete-time FIR Filter

Traditional discrete-time transversal FIR filters have been widely used in hard disk read channel equalization [25–27] and in broadband modems equalizer [28]. Depending on the circuit realization of tap delay line and multiplier, the discrete-time FIR filters can be grouped into following four categories:

- Fully digital realization [29–31]
- Digital tap delay line + multiplying digital to analog converter (MDAC) [32]
- Serial sampling analog tap delay line + analog multiplier

Authorized licensed use limited to: WASHINGTON UNIVERSITY LIBRARIES. Downloaded on March 25,2025 at 20:42:53 UTC from IEEE Xplore. Restrictions apply.

- Parallel sampling analog tap delay line + analog multiplier

Structures of the first two types require high speed ADC to convert received analog signal into digital bits, which is hard to realize with CMOS technology at Gbps data rate. Tap delay line of the third type has been realized with unit gain sample-and-hold (S&H) cell. Analog input signal passes through the delay line directly and there is no need for high-speed ADC. The disadvantage of this structure is that each S&H cell introduces distortion and attenuation to the delayed signal. All distortion and attenuation due to nonlinearity, clock feed through and limited bandwidth of S&H cell will accumulate along the line [33]. Another main drawback of serial sampling delay is that each delay unit must settle down in one symbol period which requires high frequency clock and wide bandwidth S&H.

To avoid error accumulation, parallel sampling units of the fourth type sample input signal in sequence and switch them to the corresponding multipliers through rotating switch matrix [33–36]. To relieve timing constraint on settling time of S&H, extra redundant S&H units can be added. This method lowers speed requirement of S&H at the cost of additional delay and area. Instead of switching sampled analog signal, coefficient-rotating architecture shifts the digital coefficients of FIR filter [37, 38]. At each clock period, only one S&H samples the current input and all digital coefficients are shifted once to align with input data.

As charges stored on sampling capacitor can be summed up directly by short connection of all of them; parallel sampling, multiplication and summing can be realized with very compact switch-capacitor FIR filter [39–41]. Figure 18 shows the block diagram of switch-capacitor FIR filter in [41]. Since opamp works in negative feedback loop, limited bandwidth prevents this structure being used in high frequency. Figure 19 shows the schematic of 2-tap switch-capacitor FIR filter for 1.25 Gb/s data transceiver without feedback loop [42]. At clock phase $\Phi 1$, output is reset to a pre-charge voltage *Vtt* and input signals are stored on *C2*. At the next sampling phase $\Phi 2$, *C1* and *C2* are connected parallel and the output is equal to a weighted sum of previously stored sampling and the current sampling. Coefficients of FIR filter are set by ratio of two capacitance values. Dynamically adaptive FIR filter can be implemented by replacing each capacitor with a binary weighted capacitor array at the cost of lower bandwidth.

Both methods above avoid error accumulation along the line, while introducing new issues. The complexity of rotating switch matrix increases with square law of tap number, which may lead to lay out difficulty and crosstalk [38]. Coefficient-rotating architecture needs to rotate digital coefficient each clock period. This process also introduces crosstalk to analog signal and consumes lots of power. To avoid complex switching matrix and solve the settling time problems of delay unit, multiplier and adder, discrete FIR filter in high speed data transceiver uses parallel sampling + parallel multiplier structure. FIR filter in Gbps data transceiver uses only two tap symbol-rate or half symbol-rate FIR filter [17, 43]. FIR filter with more tap numbers is limited by the time margin. Figure 20 shows the block diagram of such a parallel equalizer [44]. Two adjacent outputs of demultiplexer are fed to one equalizer and subtracted using a cross-coupled transconductor, whose output current is proportional to the difference of two inputs. Therefore, FIR coefficients can be dynamically adjusted

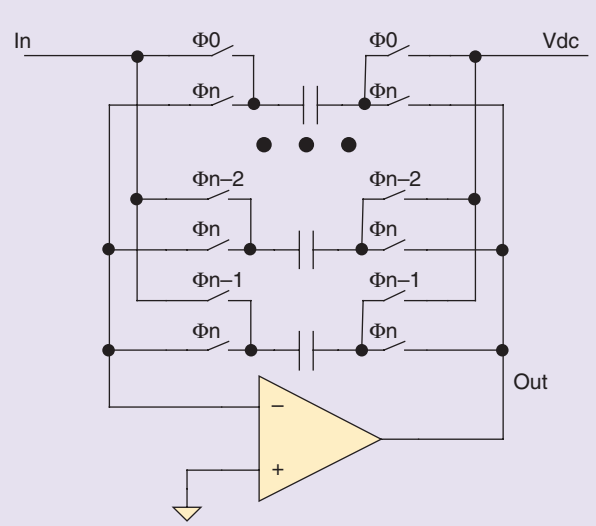

Figure 18. Discrete-time FIR filter using switch-capacitor.

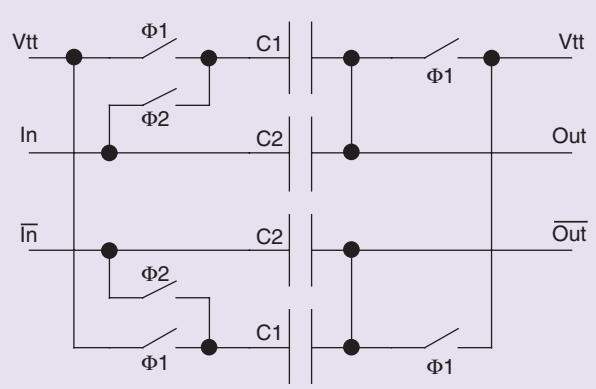

Figure 19. 2-tap switch-capacitor FIR filter for high-speed transceiver.

Authorized licensed use limited to: WASHINGTON UNIVERSITY LIBRARIES. Downloaded on March 25,2025 at 20:42:53 UTC from IEEE Xplore. Restrictions apply.

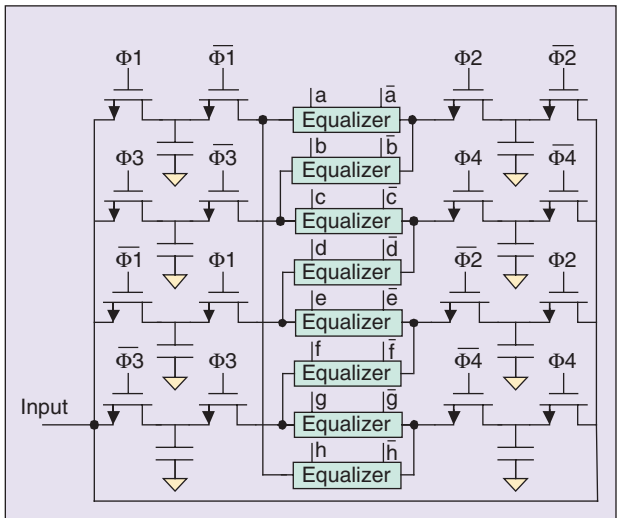

Figure 20. Demultiplexed equalizer.

by controlling the source current of transconductor. The speed requirement is relaxed by using 8 parallel equalizers. For data period T, each equalizer has 8 T time to complete one calculation.

Active Equalizer Using Continuous-time FIR Filter

Analog continuous-time delay cell [4, 45–47] has been proposed for continuous-time FIR filter design. One of the methods is to use source follower [46, 48]. However, applying active continuous-time tap delay line in higher frequency range is highly limited by the bandwidth of CMOS circuit. Artificial transmission line made of bonding wire or on-chip planar inductors have been used to increase bandwidth of distributed amplifier [49, 50]. A differential 4-tap fractionally spaced FIR filter in SiGe technology for 10 Gb/s optical receiver equalization has been reported [4]. Its transmission line composed of off-chip spiral inductors and on-chip MIM capacitors because the transmission line is too long to be realized on chip. Although artificial transmission line has shown great potential for wide bandwidth operation, it is challenging to implement high quality on-chip inductor and minimize the chip area. In [47], a 0.25-μm CMOS continuous-time 6-tap FIR filter as an 8x fractionally spaced receiver equalizer has been designed. The FIR filter has on-chip analog delay line realized with second order low pass filters; the group delay per tap is designed for 125 ps. The bandwidth with a constant group delay is tunable from 800 MHz to 2.1 GHz.

Adaptation Criteria and Related Algorithms

To adapt to the effect of variation in transmission distance and additional sockets/connectors, an error signal related to the quality of the received data must be generated to tune the transfer function of the equalization filter. Though the bit-error-rate (BER) criterion is the primary performance measurement for digital communication systems, the vast amount of data samples required for BER calculation makes it an inefficient adaptation criterion. The most widely used adaptation criterion is mean square error (MSE) calculated between the recovered signal and the training data in the time domain at sampling points. The typical equalizer structures using this criterion are feed-forward transversal equalizers (FFE) and decision-feedback equalizer (DFE) using least-mean square (LMS) algorithm or its variations. The second method obtains error signal by sampling the equalizer output waveform and then analyzing its characteristics in the time domain. The third method to generate error signal, mainly used in high-speed analog equalizers, is to use statistical spectrum information.

Minimum Mean Square Error

The minimum mean square error (MMSE) criterion tries to minimize the power of residual ISI and noise at the decision instants of received signal, which is expressed as below [51, 52]:

$$\min \varepsilon = \min \mathrm{E}[e_k^2] = \min E[(\overline{x}_k - x_k)^2],$$

where E[·] is the expectation value, $\overline{x}_k$ is equalized data and x_k is the reference data. After the training process converges or the BER is low, the reference data can be replaced by decision data [53]. The typical equalizer structures using this criterion are linear equalizer or decision feedback equalizer (DFE).

For MMSE equalizer, the matrix form of optimum transfer function is expressed as:

$$C = \Gamma^{-1}\xi,$$

where Γ is the covariance matrix of the signal samples, C is the coefficients vector of linear equalizer and ξ is coefficients vector of channel equalizer, which can be modeled using a linear equalizer. The above expression provides the analytical expression for the optimum transfer function for linear equalizer under MMSE criterion. The value C can be solved by using Levinson-Durbin algorithm to find the inverse matrix of Γ or using iterative procedure, such as steepest-descent method. The updated process of iterative procedure for coefficient vector C is:

$$\begin{aligned} C_{k+1} &= C_k - \Delta Grad_k \\ &= C_k - \Delta(-E(\varepsilon_k V_k)), \end{aligned}$$

where Δ is a constant to ensure that iterative process converges. The updated gradient $Grad_k$ is equal to the

Authorized licensed use limited to: WASHINGTON UNIVERSITY LIBRARIES. Downloaded on March 25,2025 at 20:42:53 UTC from IEEE Xplore. Restrictions apply.

expectation value of multiplication of error ε_k and V_k, the sampled vector of received data corresponding to error ε_k.

However, for practical real time digital communication, channel response is always unknown and the covariance matrix of signal sequence is not available. To overcome this difficulty, least mean square (LMS) algorithm uses the instantaneous value of $-\varepsilon_k V_k$ as updated gradient instead of its expectation value. Consequently, the coefficients updated equation for LMS algorithm is:

$$C_{k+1} = C_k + \Delta\varepsilon_k V_k$$

To speed up computation process and simplify the implementation, variations of LMS algorithm use only the sign information of ε_k (sign-error LMS or SE-LMS), the sign information of V_k (sign-data LMS or SD-LMS) or both signs information (sign-sign LMS or SS-LMS). When realized in analog circuit and in the presence of DC offset, SD-LMS and SS-LMS algorithm can diverge from the optimum gradient path and result in excess MSE. SE-LMS algorithm is most suitable for high-speed analog adaptive filters due to its simple realization and low sensitivity to DC offset [54].

Another algorithm called Sign-sign block LMS [55] can be used to reduce further the hardware implementation complexity and speed requirement; it has been used in a transmitter pre-emphasis adaptive equalizer in [12]. The weight updating algorithm is as follows:

$$C_k(j+1) = C_k(j) + sgn\left(\sum_{i=0}^{L-1} sgn(\varepsilon_{jL-1}) sgn(\varepsilon_{jL-i-k})\right).$$

Waveform Monitor

The second criterion obtains error signal by sampling the equalized output waveform and then analyzing its characteristics in time domain. For example, the value of equalized signal sampled at the peak or in the transition band can be used to decide whether it is over equalization or under equalization [56, 57]. Another example, which has been used in optical receiver, is to monitor the eye opening of the equalized signal [58]. When ISI is not severe, the received signal usually has open eyes, as in the case of optical channel and it is easy to determine the quality of the received signal by the eye opening width. However, when the transmission speed and/or the media length are increased, ISI could be very severe for coaxial cable or PCB traces, so that the received signal has closed eyes. It becomes impossible to compare the quality of two received signals when both have closed eyes.

Frequency Spectrum Error Criterion

Criteria and algorithms above need a clock with accurate sampling phase to obtain time-domain information required for error calculation. However, clock recovery loop, like PLL, needs well-equalized data to converge. These two loops are not independent and may both fail [56]. The third error criterion is to minimize statistical spectrum error [1, 59–61]. This method has several advantages over the previous methods: (a) using statistical information as adaptation criteria relaxes the speed requirement of the tuning circuit since statistical information is time-average result; (b) using continuous-time analog circuit to compare signals in frequency domain other than time domain, sampling clock with accurate phase is not needed; and (c) the desired spectrum is a statistical information and it is not necessary to have a training sequence.

For data communications with data rate higher than several hundred Mbps, the typical method to find the power spectrum is to use high-pass or bandpass filters followed by a rectifier or a squarer circuit [1, 59, 60, 62, 63]. For signals in the GHz range, the excess phase problem prevents any attempt of using a traditional Gm-C or OTA-C CMOS filter to realize bandpass filter [64]; an alternative method is to use an active inductor or gyrator to simulate passive RLC circuits [65] [66]. The main drawbacks are their small linear input range and high power consumption. In addition, they also suffer from the influence of the nonlinearity of parasitic capacitors. In [67], a method called pulse extraction has been used to estimate the power spectrum of digital signals, which is then used to generate an error signal to tune Gbps data rate equalizers for digital communications. The DC component of the pulse extraction circuit output is the weighted integration of the input signal power spectrum; the weight factor is equivalent to a bandpass filter bank. This method can be realized with standard digital circuits, thus, it is scalable to higher-speed technologies and is less sensitive to the influence of the parasitic. At the same time, the power consumption and chip area are largely reduced.

There are two other issues for applying spectrum error criterion in adaptive FIR filter. First, unlike in LMS algorithm, where the updating gradient of coefficient of the FIR filter is proportional to the multiplication of the MSE with the received signal, the power spectrum difference across the slicer is only a sign of under equalization, well equalization or over equalization. The adaptive gradient cannot be calculated from the spectrum difference and the updating gradient is unknown. Second, when the ISI is not severe, the slicer will make correct decisions most of the time, then, the slicer output is essentially equivalent to a reference signal. However, when the ISI is very severe, the slicer will make wrong decisions most of the time, then, the slicer output will not have the same statistical spectrum as the scrambled and coded random

Authorized licensed use limited to: WASHINGTON UNIVERSITY LIBRARIES. Downloaded on March 25,2025 at 20:42:53 UTC from IEEE Xplore. Restrictions apply.

data. For a well designed split-path filter, this might not be a problem since there are only two adapting directions; if the decision is mostly wrong, the signal is under equalized and increase the high frequency band gain is the right direction to go. But, for FIR filters with multiple taps, the decision is not as simple and the adaptation criterion will be misleading. In [61, 67], random-weight-change algorithm has been used to solve this problem to adapt a 6-tap FIR filter based on the spectrum criterion.

Acknowledgement

The authors wish to acknowledge the financial support from the Nation Science Foundation, Semiconductor Research Corporation, Texas Instruments, Inc., and Intel Corp. They also wish to thank Joy Li from HP Corp., David K. Johnson and Bob Payne from Texas Instruments, Inc. for their helpful discussion and reviewing of the article and Professor G. Ron Chen from City University of Hong Kong for inviting and reviewing the article.

References

[1] J.N. Babanezhad, "A 3.3 V analog adaptive line-equalizer for fast Ethernet data communication," in *Proc. IEEE Custom Integrated Circuits Conf.*, 1998, pp. 343–346.

[2] J. Cioffi, W. Abbott, H. Thapar, C. Melas, and K. Fisher, "Adaptive equalization for magnetic-disk storage channels," *IEEE Comm. Mag.*, vol. 28, pp. 14–29, Feb. 1990.

[3] M. Shtaif, "Modeling and analysis of digital optical communications systems," in *Encyclopedia of Telecommunications*, J.G. Proakis, Ed. New York: Wiley, 2003.

[4] H. Wu and J. Tierno, et al., "Differential 4-tap and 7-tap transverse filters in SiGe for 10 Gb/s multimode fiber optic link equalization," in *ISSCC Digest of Technical Papers*, pp. 180–181, 2003.

[5] H. Johnson and M. Graham, *High-Speed Signal Propagation—Advanced Black Magic*. Englewood Cliffs, NJ: Prentice Hall, 2003.

[6] W.J. Dally and J.W. Poulton, *Digital Systems Engineering*, Cambridge: Cambridge University Press, 1998.

[7] J.G. Proakis, *Digital Communications*, 4th ed., McGraw-Hill Higher Education, 2000.

[8] S.H. Hall, G.W. Hall, and J.A. McCall, *High-Speed Digital System Design*, John Wiley & Sons, Inc., 2000.

[9] M.I. Montrose, *EMC and the Printed Circuit Board: Design, Theory, and Layout Made Simple*, Piscataway, NJ: IEEE, 1998.

[10] I. Kalet and S. Shamai, "On the capacity of twisted wire pair: Gaussian model," *IEEE Trans. Comm.*, vol. 38, pp. 379–383, March 1990.

[11] Workshop on Analog Telecom and Circuit Concepts, *ISSCC*, Feb. 2003.

[12] J.T. Stonick, G.-Y. Wei, J.L. Sonntag, and D.K. Weinlader, "An adaptive PAM-4 5-Gb/s backplane transceiver in 0.25-μm CMOS," *IEEE J. Solid-state Circuits*, vol. 38, no. 3, pp. 436–443, March 2003.

[13] W.J. Dally and J. Poulton, "Transmitter equalization for 4-Gbps signaling," *IEEE Micro*, pp. 48–56, Jan./Feb. 1997.

[14] A. Fiedler, R. Mactaggart, J. Welch, and S. Krishnan, "A 1.0625 Gbps transceiver with 2x-oversampling and transmit signal pre-emphasis," in *ISSCC Digest of Technical Papers*, pp. 238–239, Feb. 1997.

[15] D.J. Foley and M.P. Flynn, "A low-power 8-PAM serial transceiver in 0.5-μm digital CMOS," *IEEE J. Solid-state Circuits*, vol. 37, no. 3, pp. 310–316, March 2002.

[16] R. Farjad-Rad, C.-K. K. Yang, M. Horowitz, and T. H. Lee, "A 0.3 μm CMOS 8-Gb/s 4-PAM serial link transceiver," *IEEE J. Solid-state Circuits*, vol. 35, pp. 757–764, May 2000.

[17] R. Farjad-Rad, C.-K. K. Yang, M. Horowitz, and T. H. Lee, "A 0.4 μm CMOS 8-Gb/s 4-PAM serial link transceiver," *IEEE J. Solid-state Circuits*, vol. 35, pp. pp. 580–585, May 1999.

[18] Maxim Integrated Products, "Designing a simple, small, wide-band and low-power equalizer for FR4 copper links," *DesignCon*, 2003.

[19] J. Addis and B. Hoffer, "Feedbeside amplifier," U.S. Patent: 4,132,958, 1979.

[20] Maxim Integrated Products, "MAX3800: 3.2 Gbps Adaptive Equalizer and Cable Driver," 2001.

[21] Y. Kudoh, M. Fukaishi, and M. Mizuno, "A 0.13 μm CMOS 5-Gb/s 10-m 28 AWG cable transceiver with no-feedback-loop continuous-time post-equalizer," *IEEE J. Solid-state Circuits*, vol. 38, no. 5, pp. 741–746, May 2003.

[22] Y. Tsividis, Z. Czarnul, and S.C. Fang, "MOS transconductors with high linearity," *Electron. Lett.*, vol. 22, pp. 245–246, Feb. 1986.

[23] J. Choi, M. Hwang, and D. Jeong, "A CMOS 3.5 Gbps continuous-time adaptive cable equalizer with joing adaptation method of low-frequency gain and high-frequency boosting," in *VLSI Technology Symp. Dig. Tech. Papers*, pp. 103–106, 2003.

[24] R. Farjad-Rad and H.-T. Ng, et al., "0.622-8.0 Gbps 150 mW serial IO macrocell with fully flexible preemphasis and equalization," in *VLSI Technology Symp. Dig. Tech. Papers*, pp. 63–66, 2003.

[25] J.E.C. Brown, P.J. Hurst, and L. Der, "A 35 Mb/s mixed-signal decision-feedback equalizer for disk drives in 2-um CMOS," *IEEE J. Solid-State Circuits*, vol. 31, no. 9, pp. 1258–1266, Sept. 1996.

[26] R. Gomez, M. Rofougaran, and A.A. Abidi, "A discrete-time analog signal processor for disk read channels," in *ISSCC Digest of Technical Papers*, pp. 212–213, 1993.

[27] P.K.D. Pai, A.D. Brewster, and A.A. Abidi, "A 160-MHz analog front-end IC for EPR-IV PRML magnetic storage read channels," *IEEE J. Solid-State Circuits*, vol. 31, no. 11, pp. 1803–1816, Nov. 1996.

[28] C.J. Nicol, P. Larsson, K. Azadet, and J.H. O'Neil, "A low-power 128-tap digital adaptive equalizer for broadband modems," *IEEE J. Solid-State Circuits*, vol. 32, no. 11, pp. 1777–1789, Nov. 1997.

[29] C.S.H. Wong, J.C. Rudell, G.T. Uehara, and P.R. Gray, "A 50 MHz eight-tap adaptive equalizer for partial-response channels," *IEEE J. Solid-State Circuits*, vol. 30, no. 3, pp. 228–234, March 1995.

[30] S. Rylov and A. Rylyakov, et al., "A 2.3 Gsample/s 10-tap digital FIR filter for magnetic recording read channels," in *ISSCC Digest of Technical Papers*, pp. 190–191, 2001.

[31] R. Staszewski, K. Muhammad, and P. Balsara, "A 550 Msample/s 8-tap FIR digital filter for magnetic recording read channels," in *ISSCC Digest of Technical Papers*, pp. 80–81, 2000.

[32] J.E.C. Brown, P.J. Hurst, and L. Der, "A 35 Mb/s mixed-signal decision-feedback equalizer for disk drives in 2-um CMOS," *IEEE J. Solid-State Circuits*, vol. 31, no. 9, pp. 1258–1266, Sept. 1996.

[33] S. Kiriaki and T.L. Viswanathan, et al., "A 160-MHz analog equalizer for magnetic disk read channels," *IEEE J. Solid-State Circuits*, vol. 32, no. 11, pp. 1839–1850, Nov. 1997.

[34] J. Sonntag, O. Agazzi, and P. Aziz, et al., "A high-speed, low power PRML read channel device," *IEEE Trans. Magnetics*. vol. 31, no. 2, pp. 1186–1195, March 1995.

[35] D. Xu, Y. Song, and G.T. Uehara, "A 200 MHz 9-tap analog equalizer for magnetic disk read channels in 0.6 um CMOS," in *ISSCC Digest of Technical Papers*, pp. 74–75, 1996.

[36] X. Wang and R.R. Spencer, "A low-power 170-MHz discrete-time analog FIR filter," *IEEE J. Solid-State Circuits*, vol. 36, no. 5, pp. 816–822, May 2001.

[37] Y.L. Cheung and A. Buchwald, "A sampled-data switched-current analog 16-tap FIR filter with digitally programmable coefficients in 0.8 μm CMOS," in *ISSCC Digest of Technical Papers*, pp. 54–55, 1997.

[38] T.-C. Lee and B. Razavi, "A 125-MHz CMOS mixed-signal equalizer for Gigabit Ethernet on copper wire," in *Proc. IEEE Custom Integrated Circuits Conf.*, 2001, pp. 131–134.

[39] G.T. Uehara and P.R. Gray, "Parallelism in analog and digital PRML magnetic disk read channel equalizers," *IEEE Trans. Magnetics*, vol. 31, no. 2, pp. 1174–1179, 1995.

[40] Z. Ciota, A. Napieralski, and J. L. Noullet, "Analogue realisation of integrated FIR fitlers," *IEE Proc.-Circuits Devices Syst.*, vol. 143, no. 5, pp. 274-281, 1996.

Authorized licensed use limited to: WASHINGTON UNIVERSITY LIBRARIES. Downloaded on March 25,2025 at 20:42:53 UTC from IEEE Xplore. Restrictions apply.

[41] N.P. Kelly, D.L. Ray, and D.W. Vogel, "A mixed-signal DFE/FFE receiver for 100Base-TX applications," in *ISSCC Digest of Technical Papers*, pp. 310–311, 2000.

[42] K. Gotoh and H. Tamura, et al., "A 2B parallel 1.25 Gb/s interconnect I/O interface with self-configurable link and plesiochronous clocking," in *ISSCC Digest of Technical Papers*, pp. 180–181, 1999.

[43] H. Tamura and M. Saito, et al., "Partial response detection technique for driver power reduction in high-speed memory-to-processor communications," in *ISSCC Digest of Technical Papers*, pp. 342–343, 1997.

[44] J.-Y. Sim and J.-J. Nam, et al., "A CMOS transceiver for DRAM bus system with a demultiplexed equalization scheme," *IEEE J. Solid-State Circuits*, vol. 37, no. 2, pp. 245–250, Feb. 2002.

[45] N.P. Sands and M.W. Hauser, et al., "A 200 Mb/s analog DFE read channel," in *ISSCC Digest of Technical Papers*, pp. 72–73, 1996.

[46] R. Alini and G. Betti, et al., "A 200-MSample/s trellis-coded PRML read/write channel with analog adaptive equalizer and digital servo," *IEEE J. Solid-State Circuits*, vol. 32, no. 11, pp. 1824–1838, Nov. 1997.

[47] X. Lin and J. Liu, "A CMOS continuous-time FIR filter for 1 Gbps cable equalizer," in *Proc. ISCAS*, May 2003, pp. 296–299.

[48] E. Burlingame and R. Spencer, "An analog CMOS high-speed continuous-time FIR filter," in *Proc. Euro. Solid-State Circuits (ESSCIRC)*, 2000.

[49] T.T.Y. Wang, *Fundamentals of Distributed Amplification*. Boston, MA: Artech, 1993.

[50] H. Ahn and D.J. Allstot, "A 0.5-8.5-GHz differential CMOS distributed amplifier," *IEEE J. Solid-State Circuits*, vol. 37, no. 8, pp. 985–993, Aug. 2002.

[51] J.W.M. Bergman, *Digital Baseband Transmission and Recording*, Dordrecht: Kluwer, 1996.

[52] E.A. Lee and D.G. Messerschmitt, *Digital Communication*, Dordrecht: Kluwer, 1994.

[53] M. Le, P. Hurst, and K. Dyer, "An analog DFE for disk drives using a mixed-signal integrator," *IEEE J. Solid-State Circuits*, vol. 34, no. 5, pp. 592–598, May 1999.

[54] A. Shoval, D.A. Johns, and W.M. Snelgrove, "Comparison of DC offset effects in four LMS adaptive algorithms," *IEEE Trans. Circuits Syst. II*, vol. 42, no. 3, pp. 176–185, March 1995.

[55] J.R. Treichler, C.R. Johnson, Jr., and M.G. Larimore, *Theory and Design of Adaptive Filters*, Englewood Cliffs, NJ: Prentice Hall, 2001.

[56] A. Shoval, O. Shoaei, K. Lee, and R. Leonwich, "A CMOS mixed-signal 100 Mb/s receive architecture for fast ethernet," in *Proc. IEEE Custom Integrated Circuits Conf.*, 1999, pp. 253–256.

[57] M. Altmann, J.M. Caia, R. Morle, M. Dunsmore, Y. Xie, and N. Kocaman, "A low-power CMOS 155 Mb/s transceiver for SONET/SDH over co-ax & fibre," in *Proc. IEEE Custom Integrated Circuits Conf.*, 2001, pp. 127–130.

[58] T. Ellermeyer, U. Langmann, B. Wedding, and W. Pöhlmann, "A 10 Gb/s eye opening monitor IC for decision-guided optimization of the frequency response of an optical receiver," in *ISSCC Digest of Technical Papers*, pp. 50–51, 2000.

[59] A.J. Baker, "An adaptive cable equalizer for serial digital video rates to 400 Mb/s," in *ISSCC Digest of Technical Papers*, pp. 174–175, 1996.

[60] S. Gondi, R. Geiger, J. Liu, J. Bareither, S. Sterrantino, and E. Pace, "A 2v low-power CMOS 125 Mbaud repeater architecture for UTP5 cables," in *Proc. Euro. Solid-State Circuits (ESSCIRC)*, 2002, pp. 571–574.

[61] X. Lin, J. Liu, and J. Fonseka, "A High speed low-noise equalization technique with improved bit error rate," in *Proc. ISCAS,* May 2002, pp. 564–567.

[62] G.P. Hartman, K.W. Martin, and A. Mclaren, "Continuous-time adaptive-analog coaxial cable equalizer in 0.5 μm CMOS," in *Proc. ISCAS,* 1999, pp. 97–100.

[63] M.H. Shakiba, "A 2.5 Gb/s adaptive cable equalizer," in *ISSCC Digest of Technical Papers*, pp. 396–397, 1999.

[64] T. Bakken and J. Choma, "Stability of a continuous-time state variable filter with Op-amp and OTA-C integrators," in *Proc. Eighth Great Lakes Symp. on VLSI*, 1998, pp. 77–82.

[65] S. Pipilos and Y. Tsividis, "Design of active RLC integrated filters with applications in the GHz range," *Electronics Letters*, vol. 30, pp. 472–474, Mar. 1994.

[66] C.Y. Wu and S.Y. Hsiao, "The design of a 3-V 900-MHz CMOS bandpass amplifier," *IEEE J. Solid-State Circuits*, vol. 32, no. 2, pp. 159–168, Feb. 1997.

[67] X. Lin and J. Liu, "Pulse extraction: A digital power spectrum estimation method for adaptation of Gbps equalizers," in *Proc. ISCAS*, May 2003, pp. 749–752.

Biographies

Jin Liu received the B.S. degree in Electronics and Information Systems from Zhongshan University in P. R. China in 1992, the M.S. degree in Electrical and Computer Engineering from University of Houston in 1995, and the Ph.D. degree in Electrical and Computer Engineering from Georgia Institute of Technology in 1999. She has been an Assistant Professor of Electrical Engineering at the University of Texas at Dallas since 1999.

Dr. Jin Liu's research interests are in high-speed communications circuits and wide-dynamic range sensor interface circuits. Current projects include adaptive equalization, clock/data recovery circuits, and line coding techniques for Gbps range data transmissions, CMOS motion detection imager, sensor interface circuits for the miniaturization of satellite instruments, and power management circuits for battery-less and wireless sensors.

Xiaofeng Lin received the B. S. degree in Physics from Tsinghua University, Beijing, China in 1997, and the M.S. degree in Electrical Engineering from University of Texas at Dallas in 2003. He is currently working toward his Ph.D degree in the same university. His research interests focus on high-speed serial-link transceivers and mixed-signal Gbps equalizers.

Authorized licensed use limited to: WASHINGTON UNIVERSITY LIBRARIES. Downloaded on March 25,2025 at 20:42:53 UTC from IEEE Xplore. Restrictions apply.